Research Article

Predicting Thailand Electricity Load Demand with Modified Fourier Series and Seasonal-Trend Decomposition Methods Using LOESS Transformation

Nikorn Saengngam*
Department of Technical Education, Faculty of Technical Education, Rajamangala University of Technology Thanyaburi, Pathum Thani, Thailand

Unchalee Tonggumnead
Department of Mathematics and Computer Science, Faculty of Science and Technology, Rajamangala University of Technology Thanyaburi, Pathum Thani, Thailand

* Corresponding author. E-mail: nikorn@rmutt.ac.th DOI: 10.14416/j.asep.2022.02.011
Received: 27 July 2021; Revised: 22 November 2021; Accepted: 29 December 2021; Published online: 22 February 2022

Abstract
Accurate long-term and midterm electricity load forecasting play an essential role in electric power system planning. Drawing on the seasonal-trend forecasting capacity of Fourier series and LOESS transformation, this paper applies modified Fourier series transformation (MFST) and modified seasonal-trend decomposition using LOESS transformation (MSTLT) to electricity load forecasting and compares the performance of two alternative models: the ARIMA(p,d,q) SARIMA(P,D,Q) model and the support vector regression (SVR) model. The data comprise monthly electricity consumption volumes between 2002 and 2019. The data between 2002 and 2018 are utilized to construct the forecasting model, while those in 2019 are employed to test the accuracy of the predicted values. The results confirm the validity of the proposed model in terms of forecasting accuracy and interpretability.

Keywords: Thailand electricity load demand prediction, Fourier series, Seasonal forecasting model, Seasonal-trend decomposition, LOESS

1 Introduction

The Thai government strives to turn all metropolises into smart cities to enhance its citizens' quality of life. One factor playing a crucial role in the design and development of smart cities in the planning of electricity capacity. To this end, efforts have been concentrated on technological advancement, most notably the construction of smart grids that efficiently respond to electricity demand and consumption in a real-time manner through the incorporation of computerized databases and complex analytical mechanisms [1].

Not only will smart grids responsive to ever-changing electricity demand and consumption contribute to electricity capacity planning and management efficiency, but they will also ensure reliability and safety from the power generation process, through transmission, to the distribution stage. All of this requires accurate electricityloaddemand prediction drawing on meticulously chosen mathematical models.

In electricity load demand prediction, the most commonly applied models are the generalized estimating equation (GEE) and the linear mixed-effects model (LMM) for medium-term prediction [2]; the artificial neural network (ANN), for short-term prediction [3]; the integration of the generalization capability of the ANN into the Monte Carlo simulation method to enhance prediction efficiency [4]; and the recurrent artificial neural network (RANN), as exemplified in a study on short-term residential load forecasting based on a Long Short-Term Memory Network (LSTM)

recurrent neural network (RNN) [5] and a report on medium-term load pattern forecasting applying RANN [6].

Theoretically, prediction models need to address the data insufficiency and inaccuracy problems inherent in long-term prediction by disregarding seasonal elements [7]. In practice, however, taking seasonal factors into consideration is inevitable since electricity consumption is perennial throughout the year. A mathematical model basing the future on past time-series data that has gained in popularity is the autoregressive integrated moving average (ARIMA) model. As its name suggests, the ARIMA model comprises three types of time series, namely autoregressive (AR), integrated (I), and moving average (MA). Central to the model are the stationary properties, i.e., stationary means and variances of the time-series data under investigation, and the application of the Box-Jenkins method drawing on the autocorrelation function (ACF) and the partial autocorrelation function (PACF). The goals of this approach are to eliminate noise from the data, minimize errors, ensure data reliability, and ultimately maximize forecasting efficiency [8].

Further development of the ARIMA model is the seasonal autoregressive integrated moving average (SARIMA) model [9], attributable to the resemblance between seasonal influence and the sine and cosine trigonometric function movements. In one of his studies, [10] presented an SVR model hybridized with empirical mode decomposition (EMD) for electricity load forecasting. The principle is to separate the components of a time series into a number of intrinsic mode functions (IMFs) along with a remainder, where EMD forecasting systems considered both the accuracy and comprehensibility of the forecasting results. This method can be applied to unbalanced data and very complex systems and can isolate non-linear and stationary signal components. However, this method is suitable only for 1-dimensional data, i.e., data in the XY plane. [11] proposed a forecasting method called PEM & LSSVR-CCPSO, involving dividing data into two components: a periodic term and a non-linear term. The periodogram estimation method (PEM) is implemented to forecast the periodic term, while the least squaressupport vector regression (LSSVR) model is used to forecast the non-linear term. The chaotic cloud particle swarm optimization (CCPSO) algorithm is used to optimize the parameters of the LSSVR model. However, LSSVR techniques often encounter problems related to the selection of kernel functions to transform non-linear data into linear data. [12] developed a hybrid chaotic cloud quantum bats algorithm (CCQBA) to optimize non-linear dynamic algorithms. It is shown to be more effective than other methods in solving complex problems. [13] incorporated sine and cosine waves in demonstrating the movement of one cycle of the time-series Y_t at the highest or the lowest value k, where k represents the k harmonic of ω. Evidently, such a regression analysis depends on trigonometric wave functions rather than researcher discretion in giving accounts of seasonal movements provided that the time-series data in question feature movements resulting from seasonal influences. However, a caveat is in order: over-reliance on trigonometric variables and parametric estimation with the least-squares method attaching an equal weight to each observed value may produce unsatisfactory prediction outcomes. Subsequently, [14] constructed seasonal and trend decomposition (STL) using locally estimated scatterplot smoothing (LOESS). STL is a versatile and robust method for decomposing time-series data, while LOESS is a nonparametric regression that uses a weighting function with the effect that the influence of a neighboring value on the smoothed value at a certain position decreases with its distance to that position.

Concerning the assumptions underlying the development of a prediction model, [15] postulates that the data must feature a normal distribution, homoskedasticity, and non-autocorrelation. To convert data from one format to another that better fulfills these requirements, several data transformations, such as logarithmic, square, square-root, and inverse, are commonly performed. Other approaches involve deriving the square of the value of the existing data or obtaining a square value based on the criterion set from the relationships between the variances proportional to the population mean [16].

The objective of this research is to present two methods for forecasting electricity load demand time-series data. The first is the modified Fourier series transformation (MFST) model. To ensure model construction rigor, seasonal elements are tightly regulated by restricting the number of trigonometric variables. The second is the modified seasonal and

trend decomposition using LOESS transformation (MSTLT). This method can create a regression line along a particular area of data that can change angles or directions according to a non-linear data pattern.

The rest of this paper is organized as follows: In Section 2, the materials and method, the MFSL forecasting model, the MSTLT forecasting model, and the assumptions relating to data and forecasting evaluation methods are detailed. In section 3, the results and a comparison of the performance of the proposed model and other forecasting methods are presented. The conclusion is provided in Section 4.

2 Materials and Methods

The present study focuses on the development of a forecasting model for time-series data comprising trend and seasonal elements using transformation methods to ensure a normal distribution and homoskedasticity of the data. Also, decomposition methods are adopted to decompose the time-series data into the trend, seasonal, and irregular elements in additive and multiplicative forms. After that, MFST and MSTLT are applied. Additionally, the primary assumptions relating to the data and the criteria for evaluating the efficiency of the model are established.

2.1 *Modified Fourier Series Transformation (MFST)*

Modeling with the MFST method comprises four components: Fourier series for seasonal time series; the determination of k for Fourier series with a periodogram; the determination of additive and multiplicative seasonal trend models, and the MFST algorithm.

2.1.1 Fouries series for seasonal time series

Use of the Fourier series model for time-series data as a tool to explain the seasonal movement in the form of sine and cosine waves dates back to the introduction of the preliminary equation for Fourier series by [13] as follows:

$$Y_t = \lambda + \sum_{i=1}^{k} A_i \cos\left(\omega_i t - \omega_i \theta_i\right) + \varepsilon_t. \quad (1)$$

Where λ represents the time-series data average

A represents the amplitude of the data $\omega = \frac{2\pi f}{n}$ with ω representing the Fourier frequency

t represents the independent time variables and equals 1,2, …, n

θ represents the phase

i represents the number of cycles and equals 1,2, …, k

k represents the highest or lowest number of cycles in the time series n with the highest value of $\frac{n}{2}$ when n is an even number and the highest value of $\frac{n+1}{2}$ when n is an odd number.

ε represents the errors and $\varepsilon \sim \text{NIID}(0,\sigma^2)$.

In terms of the regression model, the Equation (1) can be rewritten as:

$$\cos\left(\omega t - \omega\theta\right) = \cos\omega t \cos\omega\theta + \sin\omega t \sin\omega\theta \quad (2)$$

Both sides of Equation (2) are multiplied by A to derive:

$$A\cos\left(\omega t - \omega\theta\right) = A\cos\omega t \cos\omega\theta + A\sin\omega t \sin\omega\theta \quad (3)$$

λ is added to both sides of Equation (3) to obtain:

$$\lambda + A\cos\left(\omega t - \omega\theta\right) = \lambda + A\cos\omega t \cos\omega\theta + A\sin\omega t \sin\omega\theta \quad (4)$$

$Y_t = \lambda + A\cos\left(\omega t - \omega\theta\right)$, $\alpha = A\cos\omega\theta$

$\beta = A\sin\omega\theta$ are assigned to Equation (4) to derive:

$$Y_t = \lambda + \alpha\cos\omega t + \beta\sin\omega t \quad (5)$$

Accounting for the i term, Equation (5) is transformed into [Equation (6)]:

$$Y_t = \lambda + \sum_{i=1}^{k}\left(\alpha_i \cos\omega_i t + \beta_i \sin\omega_i t\right) + \varepsilon_t, \quad (6)$$

or

$$Y_t = \lambda + \sum_{i=1}^{k}\left(\alpha_i \cos\frac{2\pi i t}{n} + \beta_i \sin\frac{2\pi i t}{n}\right) + \varepsilon_t. \quad (7)$$

2.1.2 Periodogram

The seasonal component is defined using Equation (7), while a periodogram is a tool to determine the appropriate k values. A periodogram is a function of f_i in the form of $h(f_i) = \frac{n}{2}(\alpha_i^2 + \beta_i^2)$, where i equals 1,2, …, k. In the event that the f value is between 0 and 0.5,

the $h(f)=\frac{n}{2}(\alpha^2+\beta^2)$ function will take the form of a spectrum. To determine the periodic value of a season, the spectral density or Fourier transformation of autocorrelation can be estimated with the following Equation (8):

$$I(f)=2\left(1+\sum_{k=1}^{\infty}\rho_k\cos(2\pi fk)\right), \quad (8)$$

where $0 \le f \le 0.5$.

2.1.3 Determination of additive and multiplicative seasonal trend models

Modified seasonal-trend decomposition using Fourier as a time-series is made up of seasonal, trend, cyclical, and irregular components while other elements are eliminated. With regard to a forecasting model with data comprising seasonal and trend elements, the linear trend is determined as Equation (9):

$$Y_t=\beta+\beta_1 t+e_t. \quad (9)$$

Where Y_t represents the observed values in the time series

t represents time and equals 1,2,…, n

β and β_1 represent the parameters of the linear trend model

e_t represents the errors

In the event that a time series is in the form of an additive seasonal trend, the trend-adjusted time series derived will be $y_t=Y_t-\hat{Y}_t=Y_t-\hat{\beta}_0-\hat{\beta}_1 t$. As for a multiplicative seasonal trend, the trend-adjusted time series obtained will be $y_t=\frac{Y_t}{\hat{Y}_t}=\frac{Y_t}{\hat{\beta}_0+\hat{\beta}_1 t}$ with y_t being employed to develop the seasonal components of the model through a Fourier series transform. In [17], the highest i value is determined as L, where L represents the number of seasons. Therefore, the seasonal adjustment of (7) above results in the following equation:

$$y_t=\lambda+\sum_{i=1}^{L}\left(\alpha_i\cos\frac{2\pi it}{n}+\beta_i\sin\frac{2\pi it}{n}\right)+\varepsilon_t. \quad (10)$$

However, the formation of Equation (10) with $i = L = 12$ can lead to an excessively smooth model that does not fit the time-series data in cases where they are collected over a long period of time with seasonal movements, such as monthly for 20 years. To overcome this problem and sufficiently account for seasonal influences, the model is constructed from the time-series y_t and the number of cycles i, where i = 1,2,..., q and q represents the appropriate number of cycles that maximizes the spectral density in determining the seasonal periodic value L, and hence $i = Max(q,L)$ in Equation (10). In this study, the seasonal models from Equation (7) are Equations (11) and (12):

$$y_t=\lambda+\sum_{i=1}^{L}\left(\alpha_i\cos\frac{2\pi it}{n}+\beta_i\sin\frac{2\pi it}{n}\right)+\varepsilon_t, \text{ where L > q.} \quad (11)$$

and

$$y_t=\lambda+\sum_{i=1}^{q}\left(\alpha_i\cos\frac{2\pi it}{n}+\beta_i\sin\frac{2\pi it}{n}\right)+\varepsilon_t, \text{ where q > L.} \quad (12)$$

As for a Fourier series model for time-series decomposition, [18] determined the additive and multiplicative seasonal trends as $\hat{Y}_t=\hat{\beta}_0+\hat{\beta}_1 t+(\hat{y}_t)$ and $\hat{Y}_t=\left(\hat{\beta}_0+\hat{\beta}_1 t\right)(\hat{y}_t)$, respectively.

Therefore, additive models accounting for the seasonal trend can be obtained using Equations (13) and (14):

$$\hat{Y}_t=\hat{\beta}_0+\hat{\beta}_1 t+\sum_{i=1}^{L}\left(\lambda+\alpha_i\cos\frac{2\pi it}{n}+\beta_i\sin\frac{2\pi it}{n}\right), \text{ where L > q.} \quad (13)$$

and

$$\hat{Y}_t=\hat{\beta}_0+\hat{\beta}_1 t+\sum_{i=1}^{q}\left(\lambda+\alpha_i\cos\frac{2\pi it}{n}+\beta_i\sin\frac{2\pi it}{n}\right), \text{ where q> L.} \quad (14)$$

Also, multiplicative models taking into account the seasonal trend can be derived using Equations (15) and (16):

$$\hat{Y}_t=\left(\hat{\beta}_0+\hat{\beta}_1 t\right)\left(\sum_{i=1}^{L}\left(\lambda+\alpha_i\cos\frac{2\pi it}{n}+\beta_i\sin\frac{2\pi it}{n}\right)\right), \text{ where L > q .} \quad (15)$$

and

$$\hat{Y}_t=\left(\hat{\beta}_0+\hat{\beta}_1 t\right)\left(\sum_{i=1}^{q}\left(\lambda+\alpha_i\cos\frac{2\pi it}{n}+\beta_i\sin\frac{2\pi it}{n}\right)\right), \text{ where q > L.} \quad (16)$$

2.1.4 MFST algorithm

The MFST modeling process involves transforming time-series data, estimating the trend component using a linear trend, adjusting the trend from the time series, determining the appropriate k values for the Fourier series, constructing the seasonal model, and creating the final model by combining the trend and seasonal components in additive and multiplication forms. The details of the MFST algorithm are displayed in Figure 1.

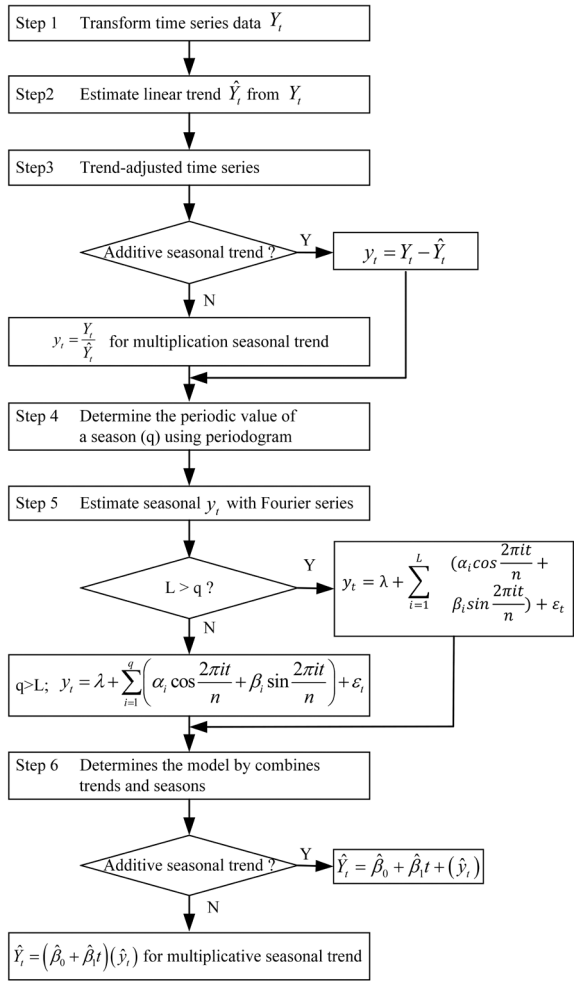

Figure 1: Modified Fourier series transformation (MFST) algorithm flowchart.

2.2 *Modified Seasonal-Trend Decomposition Using LOESS Transformation (MSTLT)*

This section applies the LOESS regression function in estimating the trend component. The trend decomposition applies the STL method. After that, the trend component from the STL method is used to create a model using the MSTLT method, as presented in Section 2.2.3.

2.2.1 LOESS regression

LOESS is a method developed to solve outlier problems that may impact the construction of a trend equation, by locally smoothing the data in a regression function through weighting. Thus, the patterns and features of the data govern the regression curve with the weighted function addressing the distance between an observed value Y_t and a neighboring point Y_k, where k = 1,2,…,m. As a result, the weighted function is represented as:

$$w(t_k) = \left(1 - \left|\frac{t_i - t_k}{d_i}\right|^3\right)^3 \text{ with } k = 1,2,\ldots,m$$

Where t_i represents the time variable at time i, i = 1,2,…,n, which is an independent variable

t_k represents the point under consideration m in proximity to t_i

d_i represents the distance between t_i and m, with the greatest distance being equal to Y_t and the smallest distance being equal to 0

A linear regression derived by the LOESS method is in the form of a quadratic function that estimates parametric values using the least squares method. As it is possible that regression function estimation may be affected by an outlier, the LOESS method assigns a robust weight to such an outlier with:

$$G(t_k) = \left(1 - \left(\frac{\left|Y_t - \hat{Y}_t\right|}{6 \text{ median}\left(\left|Y_t - \hat{Y}\right|\right)}\right)^2\right)^2, \text{ for } \left|\frac{\left|Y_t - \hat{Y}_t\right|}{6 \text{ median}\left(\left|Y_t - \hat{Y}\right|\right)}\right| < 1$$

$$, \text{ for } \left|\frac{\left|Y_t - \hat{Y}_t\right|}{6 \text{ median}\left(\left|Y_t - \hat{Y}\right|\right)}\right| \geq 1$$

In applying a robust weight, $G(t_k)$ is set at 0 if the outlier is equal to or greater than 6 times the median of the outlier, with $G(t_k)$ being multiplied by $w(t_k)$. The

estimation of each range of a linear regression function takes the form of $\sum_{k=1}^{m} w(t_k)G(t_k)(Y_k - a - bt_k - ct_k^2)^2$, which can be iterated as many times as deemed appropriate to enhance the accuracy of the curve adjustment.

2.2.2 Seasonal and trend decomposition using LOESS (STL)

Seasonal-trend decomposition using LOESS (STL) is a robust method of time series decomposition often used in economic and environmental analyses. The STL method uses a locally fitted regression model to decompose a time-series into trend, seasonal, and remainder components. This non-parametric statistic is based on the principle of estimating each component of a time series through an iterative process and is thus applicable to any form of time-series data, be it daily, weekly, monthly, or yearly. In addition, the STL algorithm performs smoothing on a time series using LOESS in two loops: the inner loop for seasonal and trend component smoothing, and the outer loop to minimize the effects of an outlier. The three components of STL analysis relating to the raw time series for an additive model is as follows:

$$Y_t = T_t + S_t + S_t$$

The three components of STL analysis relating to the raw time series for a multiplicative model are as follows:

where: Y_t represents the value of the time series at time t

T_t represents the value of the trend component at time t

S_t represents the value of the seasonal component at time t.

S_t is the value of the remainder component at time t.

2.2.3 MSTLT algorithm

This study develops a modified seasonal-trend decomposition method using LOESS transformation (MSTLT), applying STL in decomposing time series by extracting the trend component from the time series. However, the trend component obtained from the process ($T_{t(STL)}$) needs to be smoother, a further calculation is conducted with the MSTLT method to construct a trend-restricted time series, as shown in Equation (17):

$$Y(adj\ T_{t(STL)}) = Y_t - T_{t(STL)} \quad (17)$$

where $Y(adj\ T_{t(STL)})$ represents a trend-restricted time series

Y_t represents time-series data

$T_{t(STL)}$ represents the trend component from the STL method.

From the trend-restricted time series in Equation (17), it is possible to determine the average of the time-series in each quarter $\overline{Y}_i(adj\ T_t)$ and the total average of the time-series $\overline{Y}(adj\ T_{t(STL)})$, where $\overline{Y}(adj\ T_{t(STL)}) = \sum_{t=1}^{n} \frac{Y_t adj\ T_{t(STL)}}{n}$ and n represents the size of the time series.

The determination of the effect size of a season S_i for an additive seasonal model can be done by identifying the difference between the average of the time series in each quarter and the total average of the time series, as shown in Equation (18):

$$S_i = \overline{Y}_i(adj\ T_t) - \overline{Y}(adj\ T_t) \quad (18)$$

Also, the seasonal index S_i of a multiplicative seasonal model can be determined using Equation (19):

$$S_i = \frac{\overline{Y}_i(adj\ T_t)}{\overline{Y}(adj\ T_t)} \quad (19)$$

The determination of the final trend component T_t for an additive seasonal model can be done by identifying a seasonally adjusted time-series value, as shown in Equation (20):

$$T_t = Y_t - S_i \quad (20)$$

Where S_i represents the effect size of the season derived from Equation (18).

Additionally, the seasonal index T_t of an additive seasonal model can be determined using Equation (21):

$$T_t = \frac{Y_t}{S_i} \quad (21)$$

Where S_i represents the effect size of the season derived from Equation (19).

The components derived from Equations (20) and (21) are further utilized to analyze the graphically represented trend movement and construct a trend

equation fitting the data. The final step in constructing the forecasting model involves integrating the components of the trend equation and the effect size of the season in both the multiplicative and additive seasonal forms.

2.3 *Assumptions regarding the data and forecasting evaluation methods*

To fulfill assumptions relating to a normal distribution and homoskedasticity and to ensure the accuracy of the predicted value, this study applies the principles relating to the relationships between the natural logarithms of standard deviations and means constituting the data in each year proposed by [19] as follows:

$$ln\hat{\sigma}_j = \hat{a}_0 + \hat{a}_1 ln\overline{Y}_j. \quad (22)$$

Where j represents the number of years in the time-series data and equals 1,2, …, p

$\hat{\sigma}_j$ represents the standard deviation estimate of the j^{th} year

$\overline{Y}_j$ represents the mean estimate of the jth year

$\hat{\alpha}_0$ and $\hat{\alpha}_1$ represents the parameter estimates of the regression model

The absence of statistically significant relationships between the independent and dependent variables in Equation (22) is an indicator of normally distributed data. The most popular transformation for this is the Box-Cox transformation, which is in the form of:

$$Y(\lambda) = \begin{cases} \dfrac{Y^{\lambda}-1}{\lambda} & \text{, where } \lambda \neq 0. \\ ln(y) & \text{, where } \lambda = 0. \end{cases}$$

The appropriate λ is the value that maximizes the logarithm of likelihood function, as shown in:

$$f(Y_t,\lambda) = -\frac{n}{2}\ln\left(\sum_{t=1}^{n}\frac{(Y_t(\lambda)-\overline{Y}(\lambda))^2}{n}\right)+(\lambda-1)\ln(Y_t),$$

where $\overline{Y}(\lambda)=\sum_{t=1}^{n}\frac{Y_t(\lambda)}{n}$ [20].

The Bartlett's test (χ_0^2) for constant variance assumption in the transformed data also needs to be considered, as in:

$$\chi_0^2 = \frac{(n-p)\ln\hat{\sigma}_p^2 - \sum_{j=1}^{p}(n_j-1)\ln\hat{\sigma}_j^2}{1+\frac{1}{3(p-1)}\left(\sum_{j=1}^{p}\frac{1}{n_j-1}-\frac{1}{n-p}\right)}.$$

Where $\hat{\sigma}_j^2$ is the estimate of the variance for the jth year

$\hat{\sigma}_p^2$ is the estimate pool variance $\hat{\sigma}_p^2 = \frac{\sum_{j=1}^{p}(n_i-1)\hat{\sigma}_j^2}{n-p}$, p is the number of year, n_j is the sample size of time series for the jth year, and $n=\sum_{j=1}^{p}n_i\cdot\chi_0^2$ approximately follows a Chi-square distribution with p – 1 degree of freedom [21]. Once the model is derived, its predictive power is tested with the Theil's coefficient. The coefficient is obtained by:

$$U = \frac{\left(\sum_{i=1}^{n}(P_i-A_i)^2\right)^{1/2}}{\left(\sum_{i=1}^{n}A^2\right)^{1/2}}.$$

Where A_i and P_i are the ith actual and predicted values of the series, respectively. The coefficient U ranges between 0 and 1 with 0 indicating a perfect prediction, a value approaching 0 indicating a high degree of predictive accuracy, a value approaching 1 indicating a low degree of predictive accuracy, and 1 indicating a perfect inequality between the predicted values and the actual data [22].

3 Results and Discussion

The data comprise monthly electricity consumption volumes between 2002 and 2019 [23], with those between 2002 and 2018 being utilized to develop the forecasting model and those in 2019 being employed to test the predictive power of the model.

Figure 2(a) displays the time-series movements comprising seasonal and trend elements. The test to verify a normal distribution demonstrates that the data are not normally distributed at the significance level of 0.05 with the K-S test statistic value equaling 0.062 (p-value = 0.044), as illustrated in Figure 2(b). The λ value stands at –0.31 with the rounded value being –0.50, as shown in Figure 2(c). Since the data need to be converted into the form of $\frac{1}{\sqrt{Y}}$ [20], seven transformations such as $A_t=\sqrt{Y_t}$, $B_t=Y_t^{1/3}$, $C_t=Y_t^{1/4}$, $D_t=\ln Y_t$, $E_t=\frac{1}{\sqrt{Y}}$, $F_t=\frac{1}{Y_t^{1/3}}$, and $G_t=\frac{1}{Y_t^{1/4}}$ are conducted, as shown in Table 1 below.

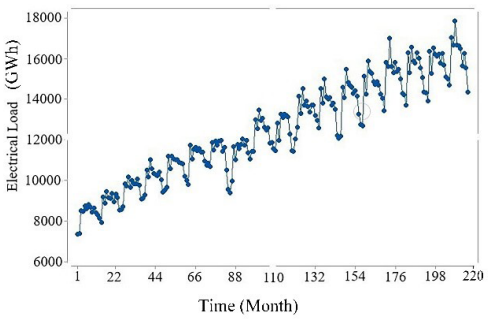

(a)

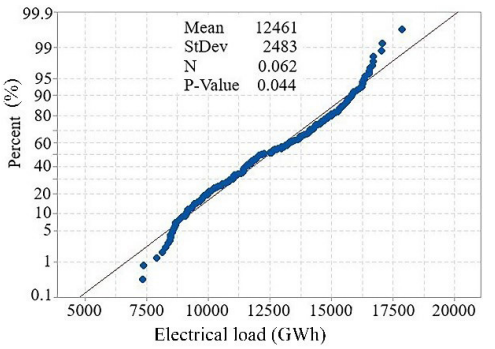

(b)

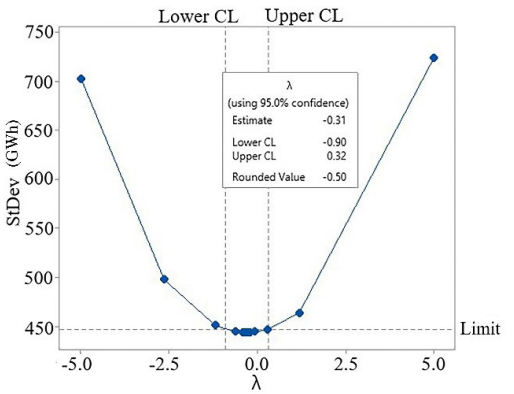

(c)

Figure 2: (a) Time-series movements, (b) Verification of the normal distribution of the data, and (c) Determination of the appropriate λ value with the Box-Cox transformation method.

Table 1 presents the types of data transformation contributing to a normal distribution proposed by [19] that involves the determination of the relationships between the natural logarithms of the estimated standard deviation for j^{th} year data ($ln\hat{\sigma}_j$) and the average of the year j^{th} of the different variables in a simple linear regression. The present research applies the original time-series data Y_t and 7 forms of data transformation, namely A_t, B_t, C_t, D_t, E_t, F_t, and G_t. Subsequently, hypothesis testing is carried out using the t-test statistic. Similar to testing whether a slope value equals 0, the simple linear regressions resulting in statistical insignificance demonstrate that the corresponding data transformations achieve a normal distribution. The findings from Table 1 suggest that when the data distribution is viewed in terms of the relationships between the natural logarithms of the estimated standard deviations for the j^{th} year data and the means constituting the data in each year in the form of a simple linear regression, the transformations $D_t = \ln Y_i$ ($t = 0.68$, p-value = 0.51), $F_t = \frac{1}{Y_t^{1/3}}$ ($t = 1.65$, p-value = 0.12), $G_t = \frac{1}{Y_t^{1/4}}$ and $t = 1.08$, p-value = 0.28) yield statistically insignificant relationships between the independent and dependent variables. Thus, such forms of data transformation lead to a normal distribution. As for Bartlett's test used to test the homoskedasticity of the transformed data, statistical insignificance indicates fulfillment of such a requirement [16], [24], [25]. According to Table 1, the values obtained from Bartlett's test range between 0.20 and 22.10 with the p-value falling between 1.00 and 0.18, suggesting statistical insignificance and thus the homoskedasticity of the data in the form of Y_t and the data transformed into A_t, B_t, C_t, D_t, E_t, F_t, and G_t. However, when the data take the form of the observed value of the original time series Y_t , the p-value was the lowest at 0.18.

Table 1: Transformations to determine the relationships between the natural logarithms of the standard deviations and means constituting the data in each year

Model	Regression	t-test	P	Bartlett's test	P
Y_t	$\ln\hat{\sigma}_j = -4.02 + 1.128\overline{Y}_j$	8.26	0.00	22.10	0.18
$A_t = \sqrt{Y_t}$	$\ln\hat{\sigma}_j = -4.56 + 1.226\overline{A}_j$	4.36	0.00	10.25	0.89
$B_t = Y_t^{1/3}$	$\ln\hat{\sigma}_j = -5.00 + 1.354\overline{B}_j$	3.03	0.01	8.27	0.96
$C_t = Y_t^{1/4}$	$\ln\hat{\sigma}_j = -5.26 + 1.462\overline{C}_j$	2.44	0.03	7.33	0.98
$D_t = \ln Y_t$	$\ln\hat{\sigma}_j = -4.97 + 0.930\overline{D}_j$	0.68	0.51	0.20	1.00
$E_t = \frac{1}{\sqrt{Y_t}}$	$\ln\hat{\sigma}_j = -4.27 + 0.831\overline{E}_j$	2.78	0.01	8.08	0.97
$F_t = \frac{1}{Y_t^{1/3}}$	$\ln\hat{\sigma}_j = -4.27 + 0.733\overline{F}_j$	1.65	0.12	6.13	0.99
$G_t = \frac{1}{Y_t^{1/4}}$	$\ln\hat{\sigma}_j = -5.03 + 0.64\overline{G}_j$	1.08	0.28	5.60	0.99

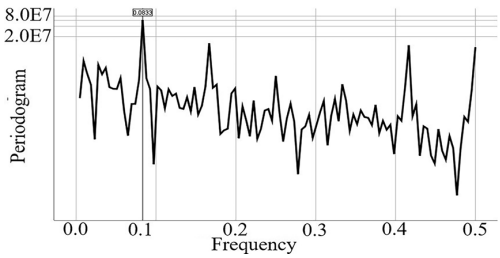

(a)

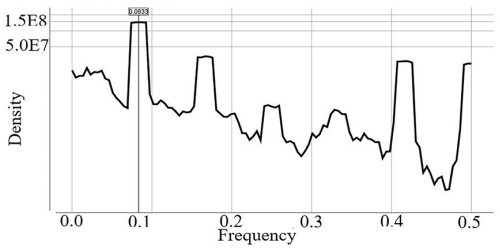

(b)

Figure 3: (a) Periodogram plot of Y_t, and (b) Spectral Density of Y_t.

Iwok [17], determines the appropriate number of cycles for the seasonal elements in the form of a Fourier series as L, where the number of years from which the data are collected is lower than the number of seasons. In the present study, this is generalized with the appropriate number of cycles being the maximum value between q and L, where q represents the appropriate number of cycles that maximizes the spectral density and L represents the number of seasons. After that, the f_i value contributing to the highest spectral density is determined.

From Figure 3, the f_i value yielding the highest spectral density is 0.0833 ($f_i = \frac{i}{n} = \frac{17}{204} = 0.0833$), q = 17, and L = 12 ($L = \frac{n}{q} = \frac{204}{17} = 12$). Since $q > L$, the additive and multiplicative seasonal time series can be determined using Equations (23) and (24), respectively.

$$\hat{Y}_t = \hat{\beta}_0 + \hat{\beta}_1 t + \sum_{i=1}^{17}\left(\lambda + \alpha_i \cos\frac{2\pi i t}{n} + \beta_i \sin\frac{2\pi i t}{n}\right). \quad (23)$$

$$\hat{Y}_t = (\hat{\beta}_0 + \hat{\beta}_1 t)\sum_{i=1}^{17}\left(\lambda + \alpha_i \cos\frac{2\pi i t}{n} + \beta_i \sin\frac{2\pi i t}{n}\right). \quad (24)$$

The seasonal-trend decomposition using Fourier series transformations is shown in Table 2. For all the transformations employed to convert the trend equations constructed in the form of a linear trend, the dependent variables vary according to time with the p-value equaling 0.0000 and the R^2 value ranging between 0.89 and 0.91. Additionally, the determination of the additive seasonal trend and the multiplicative seasonal trend results in the trend-adjusted time-series $y_t = Y_t - \hat{\beta}_0 - \hat{\beta}_1 t$ and $y_t = \frac{Y_t}{\hat{\beta}_0 + \hat{\beta}_1 t}$, respectively. Then y_t is utilized to identify the seasonal components of the model using the Fourier series method, as in Equation (12). After that, the trend and seasonal elements of the model are integrated into the additive seasonal trend and the multiplicative seasonal trend, as in Equations (23) and (24), respectively.

Table 2: Trend equations from various transformations, R^2, and slope testing

Transformations	Trend Equations	R^2	t-test for Slope	
			t	p
Y_t	$\hat{Y} = 8{,}359 + 37.815t$	0.91	45.37	0.00
$A_t = \sqrt{Y_t}$	$\hat{A}_t = 92.493 + 0.1712t$	0.91	45.25	0.00
$B_t = Y_t^{1/3}$	$\hat{B}_t = 20.4948 + 0.0238t$	0.90	44.90	0.00
$C_t = Y_t^{1/4}$	$\hat{C}_t = 9.6393 + 0.0082t$	0.90	44.68	0.00
$D_t = \ln Y_t$	$\hat{D}_t = 9.0713 + 0.0031t$	0.90	43.79	0.00
$E_t = \frac{1}{\sqrt{Y_t}}$	$\hat{E}_t = 0.0107 + 0.000014t$	0.89	–41.25	0.00
$F_t = \frac{1}{Y_t^{1/3}}$	$F_t = 0.04848 - 0.000046t$	0.89	–42.19	0.00
$G_t = \frac{1}{Y_t^{1/4}}$	$\hat{G}_t = 0.1033 - 0.00008t$	0.89	–42.63	0.00

The data transformations with the resultant additive models and Theil's coefficients are as follows:

1) Y_t transformation

$$\hat{Y}_t = (8{,}359 + 37.815t) - 180.10\cos 2\omega t - 95.40\sin 3\omega t - 158.80\sin 6\omega t + 109.30\sin 7\omega t - 1430.00\cos 2\omega t - 95.4\sin 8\omega t - 742.60\cos 17\omega t - 145.60\sin 17\omega t$$

with Theil's coefficient being 0.0312.

2) $A_t = \sqrt{Y_t}$ transformation

$$\hat{A}_t = (92.493 + 0.1712t) - 0.849\cos\omega t - 0.996\cos 2\omega t - 0.4240\cos 3\omega t - 0.5070\sin 3\omega t - 0.0069\sin 6\omega t + 0.005\sin 7\omega t - 0.006\sin 8\omega t - 0.029\cos 17\omega t - 0.007\sin 17\omega t$$

with Theil's coefficient being 0.0278.

3) $B_t = Y_t^{1/3}$ transformation

$$\hat{B}_t = (20.4948 + 0.0238t) - 0.1472\cos\omega t$$

$$-0.1473\cos 2\omega t - 0.0618\cos 3\omega t - 0.0744\sin 3\omega t$$
$$-0.1033\sin 6\omega t + 0.0715\sin 7\omega t - 0.0170\sin 8\omega t$$
$$-0.4606\cos 17\omega t - 0.0997\sin 17\omega t$$

with Theil's coefficient being 0.0274.

4) $C_t = Y_t^{1/4}$ transformation

$$\hat{C}_t = (9.6393 + 0.0082t) - 0.055\cos\omega t - 0.052\cos 2\omega t$$
$$-0.022\,\text{os}\,3\omega t - 0.026\sin 3\omega t - 0.036\sin 6\omega t$$
$$+0.025\sin 7\omega t - 0.032\sin 8\omega t - 0.158\cos 17\omega t$$
$$-0.035\sin 17\omega t$$

with Theil's coefficient being 0.0275.

5) $D_t = \ln Y_t$ transformation

$$\hat{D}_t = (9.0713 + 0.0031t) - 0.027\cos\omega t - 0.022\cos 2\omega t$$
$$-0.009\cos 3\omega t - 0.011\sin 3\omega t - 0.014\sin 6\omega t$$
$$+0.009\sin 7\omega t - 0.012\sin 8\omega t - 0.060\cos 17\omega t$$
$$-0.014\sin 17\omega t$$

with Theil's coefficient being 0.0260.

6) $E_t = \dfrac{1}{\sqrt{Y_t}}$ transformation

$$\hat{E}_t = (0.0107 - 0.000014t) + 0.00018\cos\omega t$$
$$-0.00012\cos 2\omega t + 0.00005\cos 3\omega t$$
$$+0.00006\sin 3\omega t + 0.00007\sin 6\omega t$$
$$-0.00004\sin 7\omega t + 0.00006\sin 8\omega t$$
$$+0.00027\cos 17\omega t - 0.00007\sin 17\omega t$$

with Theil's coefficient being 0.0299.

7) $F_t = \dfrac{1}{Y_t^{1/3}}$ transformation

$$\hat{F}_t = (0.04848 - 0.000046t) + 0.00051\cos\omega$$
$$+0.00015\cos 3\omega t + 0.00017\sin 3\omega t$$
$$+0.00021\sin 6\omega t - 0.00014\sin 7\omega t$$
$$+0.00018\sin 8\omega t + 0.00087\cos 17\omega t$$
$$+0.00021\sin 17\omega t$$

with Theil's coefficient being 0.0290.

8) $G_t = \dfrac{1}{Y_t^{1/4}}$ transformation

$$\hat{G}_t = (0.1033 - 0.00008t) + 0.00078\cos\omega t$$
$$+0.00056\cos 2\omega t + 0.00024\cos 3\omega t$$
$$+0.00028\sin 3\omega t + 0.00034\sin 6\omega t$$
$$-0.00022\sin 7\omega t + 0.00029\sin 8\omega t$$
$$+0.00143\cos 17\omega t + 0.00034\sin 17\omega t$$

with Theil's coefficient being 0.0279.

The data transformations with the resultant multiplicative models and Theil's coefficients are as follows:

1) Y_t transformation

$$\hat{Y}_t = (8{,}359 + 37.815t)(0.9998 - 0.0157\cos 2\omega t$$
$$-0.0099\sin 3\,\omega t - 0.0130\sin 6\,\omega t + 0.0092\sin 7\,\omega t$$
$$-0.0115\ \sin 8\ \omega t - 742.600\ \cos 17\ \omega t$$
$$-145.600\ \sin 17\ \omega t)$$

with Theil's coefficient being 0.0275.

2) $A_t = \sqrt{Y_t}$ transformation

$$\hat{A}_t = (92.493 + 0.1712t)(0.9999 - 0.0078\cos\omega t$$
$$-0.0094\sin\omega t - 0.0039\cos 3\omega t - 0.0054\sin 3\omega t$$
$$-0.0069\sin 6\omega t + 0.0046\sin 7\omega t - 0.0060\sin 8\omega t$$
$$-0.0298\cos 17\omega t - 0.0065\sin 17\omega t)$$

with Theil's coefficient being 0.0268.

3) $B_t = Y_t^{1/3}$ transformation

$$\hat{B}_t = (20.4948 + 0.0238t)(1.0000 - 0.0065\cos\omega t$$
$$-0.0067\cos 2\omega t - 0.0027\cos 3\omega t$$
$$-0.0037\sin 3\omega t - 0.0046\sin 6\omega t$$
$$-0.0031\sin 7\omega t - 0.0040\sin 8\omega t$$
$$-0.0199\cos 17\omega t - 0.0044\sin 17\omega t)$$

with Theil's coefficient being 0.0268.

4) $C_t = Y_t^{1/4}$ transformation

$$\hat{C}_t = (9.6393 + 0.0082t)(1.0000 - 0.0053\cos\omega t$$
$$-0.0050\cos 2\omega t - 0.0021\cos 3\omega t$$
$$-0.0027\sin 3\omega t - 0.0035\sin 6\omega t$$
$$+0.0023\sin 7\omega t - 0.0030\sin 8\omega t$$
$$-0.0149\cos 17\omega t - 0.0033\sin 17\omega t)$$

with Theil's coefficient being 0.0269.

5) $D_t = \ln Y_t$ transformation

$$\hat{D}_t = (9.0713 + 0.0031t)(1.000 - 0.0029\cos\omega t$$
$$-0.0009\cos 3\omega t - 0.0012\sin 3\omega t - 0.0015\sin 6\omega$$
$$+0.0010\sin 7\omega t - 0.0023\cos 2\omega t - 0.0013\sin 8\omega t$$
$$-0.0064\cos 17\omega t - 0.0015\sin 17\omega t)$$

with Theil's coefficient being 0.0258.

6) $E_t = \dfrac{1}{\sqrt{Y_t}}$ transformation

$$\hat{E}_t = (0.0107 - 0.000014t)(1.0001 + 0.0195\cos\omega t$$
$$+0.0125\cos 2\omega t + 0.0055\cos 3\omega t$$
$$+0.0048\sin 3\omega t + 0.0067\sin 6\omega t$$
$$-0.0050\sin 7\omega t + 0.0059\sin 8\omega t$$
$$+0.0304\cos 17\omega t + 0.0071\sin 17\omega t)$$

with Theil's coefficient being 0.0298.

7) $F_t = \dfrac{1}{Y_t^{1/3}}$ transformation

$$\hat{F}_t = (0.04848 - 0.00005t)(1.0001 + 0.0116\cos\omega t$$
$$+0.0080\cos 2\omega t + 0.0035\cos 3\omega t$$
$$+0.0034\sin 3\omega t + 0.0045\sin 6\omega$$
$$-0.0033\sin 7\omega t + 0.0040\sin 8\omega t$$
$$+0.0201\cos 17\omega t + 0.0047\sin 17\omega t)$$

with Theil's coefficient being 0.0300.

8) $G_t = \frac{1}{Y_t^{1/4}}$ transformation

$$\hat{G}_t = (0.10334 - 0.00008t)(1.0001 + 0.0008\cos\omega t + 0.0058\cos 2\omega t + 0.0025\cos 3\omega t + 0.0026\sin 3\omega t + 0.0034\sin 6\omega t - 0.0024\sin 7\omega t + 0.0030\sin 8\omega t + 0.0151\cos 17\omega t + 0.0035\sin 17\omega t)$$

with Theil's coefficient being 0.0284.

In [17], the model for time-series data comprising seasonal elements is developed with the seasonal elements being determined as a linear equation without data transformation, i.e., the original time-series data Y_t. In contrast, this research transforms the time-series data Y_t into seven forms, namely $A_t = \sqrt{Y_t}$, $B_t = Y_t^{1/3}$, $C_t = Y_t^{1/4}$, $D_t = \ln Y_t$, $E_t = \frac{1}{\sqrt{Y_t}}$, $F_t = \frac{1}{Y_t^{1/3}}$, and $G_t = \frac{1}{Y_t^{1/4}}$. It is found that the time series undergoing no data transformation will result in the highest Theil's coefficients for both the additive and multiplicative forms, demonstrating the lowest model efficiency. In other words, data transformation is vital to enhancing the efficiency of a forecasting model. Thiel's coefficients for the additive and multiplicative models are shown in Figure 4(a). As for the additive models, Theil's coefficient ranges between 0.0260 and 0.0312, demonstrating a high level of predictive power. Higher model efficiency at the lower Theil's coefficient of 0.0260 is achieved with a logarithmic transformation. Regarding the multiplicative models, Theil's coefficients range between 0.0258 and 0.0275, indicating again a high level of predictive power. In line with expectations, a logarithmic transformation leads to higher model efficiency at the lower Theil's coefficient of 0.0258. Figure 4(b) shows the actual data and fitted values when using the Fourier series with the multiplicative model and logarithmic transformations. This plot shows that all the plot estimates have a reasonably good value because they follow actual data pattern data. Figure 4(c) shows the autocorrelation of the residual. Further exploration of the autocorrelation of $r_k(e_t)$ converted into the form of $D_t = \ln Y_t$ shows that the errors are independent, suggesting once again that the model fares excellently in terms of its predictive power.

The result from the Fourier series demonstrates that the additive and multiplicative models from the logarithmic transformations differ very slightly. So, the logarithmic transformations and the additive model are used to construct the MSTLT forecasting model. In the present research, the strength of the LOESS regression proposed by [26] is applied to estimate the seasonal

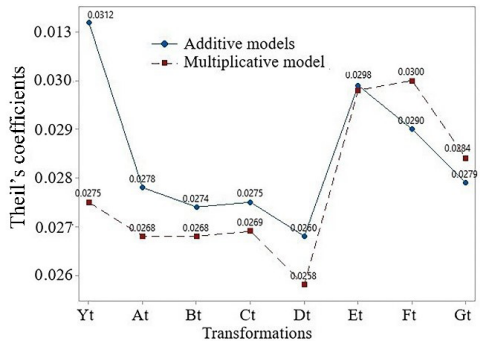

(a)

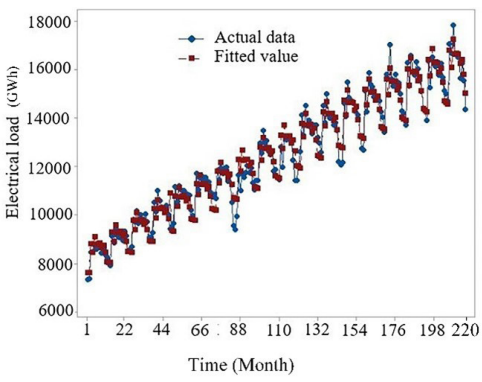

(b)

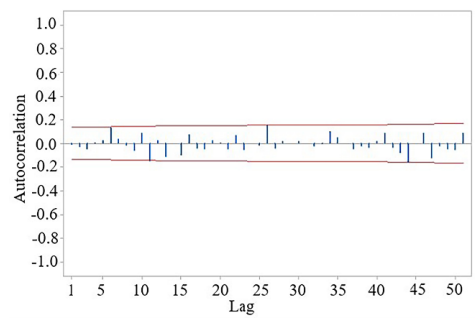

(c)

Figure 4: (a) Thiel's coefficients for the additive and multiplicative models, (b) the actual data and fitted values when using Fourier series with the multiplicative model and logarithmic transformations, and (c) autocorrelation of the residual rk(et) when using the multiplicative model and logarithmic transformation.

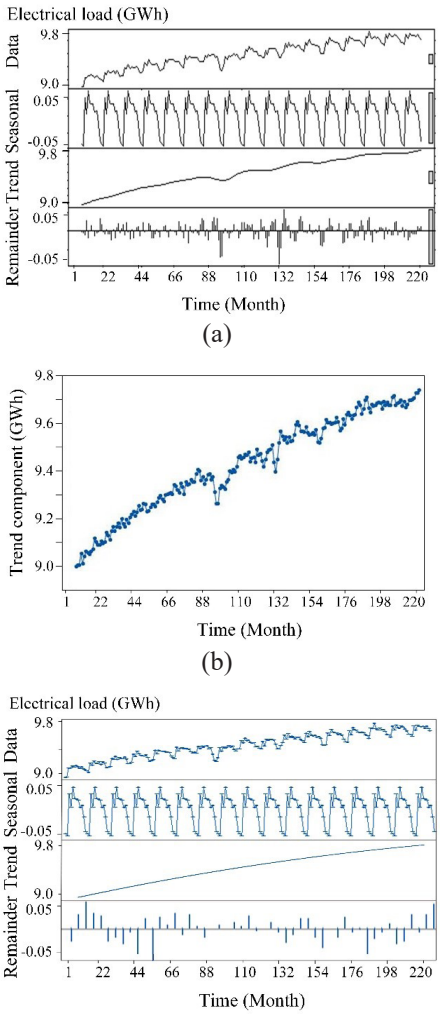

Figure 5: (a) Components of trends, seasons and irregularities when using MSTLT. (b) A new trend or de-seasonalised time series $T_t = Y_t - S_t$. (c) The components of trends, seasons, and irregularities in last step.

elements, while the STL method postulated by [27] is used to decompose seasonally, trend, and irregular elements. Also, the data are exposed to logarithmic transformations to ensure a normal distribution and homoskedasticity before the trend elements are utilized to construct the model in the form of a quadratic trend. The final components of trends, seasons, and irregularities of the modified seasonal-trend decomposition using LOESS transformation and the forecasting model are displayed in Figure 5.

From Figure 5(a), it can be seen that the trends component graph obtained by the STL method $(T_{t(STL)})$ is not as smooth. Therefore, the components of trends using STL were used to calculate the following:

1) Determine the time series adjusted trend $Y(adj\ T_{t(STL)})$ from $Y(adj\ T_{t(STL)}) = Y_t - T_{t(STL)}$.

2) Determine the total mean, $\overline{Y}(adj\ T_{t(STL)}) = 0.00023$.

3) Determine the time series adjusted trend in each seasonal, $\overline{Y}_1(adj\ T_t) = -0.0814$,

$\overline{Y}_2(adj\ T_t) = -0.0885, \overline{Y}_3(adj\ T_t) = -0.0543$,

$\overline{Y}_4(adj\ T_t) = 0.0087,\ \overline{Y}_5(adj\ T_t) = 0.0769$,

$\overline{Y}_6(adj\ T_t) = 0.0385,\ \overline{Y}_7(adj\ T_t) = 0.0365$,

$\overline{Y}_8(adj\ T_t) = 0.0334,\ \overline{Y}_9(adj\ T_t) = 0.0082$,

$\overline{Y}_{10}(adj\ T_t) = 0.0147,\ \overline{Y}_{11}(adj\ T_t) = -0.0240$,

$\overline{Y}_{12}(adj\ T_t) = -0.0746$.

Determine the seasonal influence from

$S_i = \overline{Y}_i(adj\ T_t) - \overline{Y}_2(adj\ T_t),\ \hat{S}_1 = -0.0817$,

$\hat{S}_2 = -0.0887,\ \hat{S}_3 = 0.0541,\ \hat{S}_4 = 0.0085$,

$\hat{S}_5 = 0.0766,\ \hat{S}_6 = 0.0383,\ \hat{S}_7 = 0.0363$,

$\hat{S}_8 = 0.0332,\ \hat{S}_9 = 0.0079,\ \hat{S}_{10} = 0.0145$,

$\hat{S}_{11} = -0.0242,\ \hat{S}_{12} = -0.0749$.

1) Determine a new trend or de-seasonalised time series $T_t = Y_t - S_t$., from the trend movement pattern in Figure 5(b); the quadratic trend equation can be created as :

$$\ln Y_t = 9.0190 + 0.004555\ t - 0.000007t^2 + \hat{S}_i$$

or

$$Y_t = \exp(9.0190 + 0.004555\ t - 0.000007t^2 + \hat{S}_i)$$

for $i = 1,2,\ldots,12$,

The components of trends, seasons, and irregularities in the last step are shown in Figure 5(c). The forecasting model is determined as:

$$\ln Y_t = 9.0190 + 0.004555\ t - 0.000007t^2 + \hat{S}_i$$

or

$$Y_t = \exp(9.0190 + 0.004555\ t - 0.000007t^2 + \hat{S}_i)$$

for $i = 1,2,\ldots,12$,

where, $\hat{S}_1 = -0.0817$, $\hat{S}_2 = -0.0887$, $\hat{S}_3 = 0.0541$, $\hat{S}_4 = 0.0085$, $\hat{S}_5 = 0.0766$, $\hat{S}_6 = 0.0383$, $\hat{S}_7 = 0.0363$, $\hat{S}_8 = 0.0332$, $\hat{S}_9 = 0.0079$, $\hat{S}_{10} = 0.0145$, $\hat{S}_{11} = -0.0242$, $\hat{S}_{12} = -0.074$.

The Theil' s coefficient of this method is 0.0248.

Figure 6 shows The actual data and fitted values when using MSTLT with logarithmic transformations

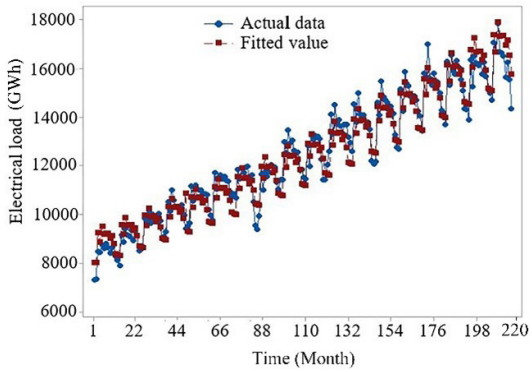

Figure 6: The actual data and fitted values when using MSTLT with logarithmic transformations and the quadratic trend.

and the quadratic trend. This plot shows that all the plot estimates have a reasonably good value because they follow actual data pattern data.

The proposed MFST and MSTLT models are compared with two alternative models, namely 1) the ARIMA(p,d,q) × SARIMA(P,D,Q) model proposed by [8] and [9], classical works widely applied to construct forecasting models for time-series data, and 2) the SVR model developed by [28], and further described in terms of efficiency by [29]. It is found that the MSTLT and MFST models outperform all other alternatives on all the evaluation criteria, and the proposed model tends to fit more closely to the actual values with a smaller forecasting error. The findings are displayed in Table 3.

Table 3: Results of the forecasting models

Methods	MAE	RMSE	MAPE
MSTL	13.965	78.298	3.064
MFS	16.060	83.593	3.189
AR*	20.573	111.439	3.273
SVR	30.924	145.780	4.400

AR* = ARIMA(p,d,q) × SARIMA(P,D,Q) model

Furthermore, to verify the significance of the accuracy improvement of the MFST and MSTLT models, a comparison between the original ARIMA(p,d,q) × SARIMA(P,D,Q) and the SVR models is conducted with the Wilcoxon signed-rank test at 0.05 significance level [30]. The test results are shown in Table 4. Clearly, the proposed MSTLT model yields a statistically significant result when compared to that obtained from the alternative models, particularly the original SVR and the ARIMA(p,d,q) × SARIMA(P,D,Q) models. The MFST model derives a statistically significant result when compared to the original SVR. In addition, the MFST model did not differ statistically from the MSTLT model.

Table 4: Wilcoxon signed-rank test

Comparisons of Models	Rank	N	Z	Sig.
MSTLT-SVR	MSTLT < SVR	11[a]	–2.432	0.015*
	MSTLT > SVR	1[b]		
MSTLT-MFST	MSTLT < MFST	10[a]	–1.883	0.060
	MSTLT > MFST	2[b]		
MSTLT-AR*	MSTLT < AR*	11[a]	–2.197	0.028*
	MSTLT > AR*	1[b]		
MFST-SVR	MFST < SVR	11[a]	–2.197	0.028*
	MFST > SVR	1[b]		
MFST-AR*	MFST < AR*	7[a]	–0.941	0.347
	MFST > AR*	5[b]		
AR*-SVR	AR* < SVR	9[a]	–1.490	0.136
	AR* > SVR	3[b]		

AR* = ARIMA(p,d,q) × SARIMA(P,D,Q) model

4 Conclusions

This study developed two models for forecasting time-series data, namely Fourier series transformation (MFST) and modified seasonal-trend decomposition using LOESS transformation (MSTLT). Based on the findings, it can be concluded that the MFST and the MSTLT models are efficient alternatives in the construction of a seasonal model, and possibly a cyclical one, for predicting the electricity load demand of Thailand and hence planning and managing the country's long-term electricity capacity. The results confirm the validity of the proposed models as forecasting methods with a high level of accuracy and interpretability. For further studies along similar lines, problems relating to the number of Fourier series and high dimensionality may be solved by parametric estimation with a penalized regression integrating a penalty function in order to achieve better model efficiency.

Acknowledgments

The author would to thank Associate Professor Dr. Krischonme Bhumkittipich and Associate Professor

Dr. Kumron Sirathanakul for their expert advice and encouragement throughout this research.

References

[1] A. C. Şerban and M. D. Lytras, "Artificial intelligence for smart renewable energy sector in europe—smart energy infrastructures for next generation smart cities," *IEEE Access*, vol. 8, pp. 77364–77377, 2020, doi: 10.1109/ACCESS.2020.2990123.

[2] N. Saengngam and U. Thonggumnead, "Predicting the medium-term electricity load demand of Thailand using the generalized estimating equation and the linear mixed effect model," in *2015 12th International Conference on Electrical Engineering/Electronics, Computer, Telecommunications and Information Technology (ECTI-CON)*, 2015, pp. 1–5, doi: 10.1109/ECTICon.2015.7206994.

[3] C. Cecati, J. Kolbusz, P. Różycki, P. Siano, and B. M. Wilamowski, "A novel RBF training algorithm for short-term electric load forecasting and comparative studies," *IEEE Transactions on Industrial Electronics*, vol. 62, no. 10, pp. 6519–6529, Oct. 2015, doi: 10.1109/TIE.2015.2424399.

[4] K. Chen, K. Chen, Q. Wang, Z. He, J. Hu, and J. He, "Short-term load forecasting with deep residual networks," *IEEE Transactions on Smart Grid*, vol. 10, no. 4, pp. 3943–3952, Jul. 2019, doi: 10.1109/TSG.2018.2844307.

[5] W. Kong, Z. Y. Dong, Y. Jia, D. J. Hill, Y. Xu, and Y. Zhang, "Short-term residential load forecasting based on LSTM recurrent neural network," *IEEE Transactions on Smart Grid*, vol. 10, no. 1, pp. 841–851, Jan. 2019, doi: 10.1109/TSG.2017.2753802.

[6] S.-M. Baek, "Mid-term load pattern forecasting with recurrent artificial neural network," *IEEE Access*, vol. 7, pp. 172830–172838, 2019, doi: 10.1109/ACCESS.2019.2957072.

[7] W. Ahmed, H. Ansari, B. Khan, Z. Ullah, S. M. Ali, C. A. Mehmood, M. B. Qureshi, I. Hussain, M. Jawad, M. U. S. Khan, A. Ullah, and R. Nawaz, "Machine learning based energy management model for smart grid and renewable energy districts," *IEEE Access*, vol. 8, pp. 185059–185078, 2020, doi: 10.1109/ACCESS.2020.3029943.

[8] G. E. P. Box and G. M. Jenkins, *Time Series Analysis: Forecasting and Control*. California: Holden Day, 1970.

[9] G. E. P. Box, G. M. Jenkins, and G. C. Reinsel, *Time Series Analysis: Forecasting and Control*. New Jersey: John Willey&Sons, 2008.

[10] G. F. Fan, S. Qing, H. Wang, W. C. Hong, and H. J. Li, "Support vector regression model based on empirical mode decomposition and auto regression for electric load forecasting," *Energies*, vol. 6, no 4, pp. 1887–1901, Apr. 2013, doi: 10.3390/en6041887.

[11] M. W. Li, J. Geng, W. C. Hong, and L. D. Zhang, "Periodogram estimation based on LSSVR-CCPSO compensation for forecasting ship motion," *Nonlinear Dynamics*, vol. 97, no. 4, pp. 2579–2594, Sep. 2019, doi: 10.1007/s11071-019-05149-5.

[12] M. W. Li, Y. T. Wang, J. Geng, and W. C. Hong, "Chaos cloud quantum bat hybrid optimization algorithm," *Nonlinear Dynamics*, vol. 103, no. 1, pp. 1167–1193, Jan. 2021, doi: 10.1007/s11071-020-06111-6.

[13] P. Bloomfield, *Fourier Analysis of Time Series: An Introduction*. New York: John Wiley & Sons, 1976.

[14] C. Robert, C. William, and T. Irma, "STL: A seasonal-trend decomposition procedure based on loess," *Journal of official statistics*, vol. 6, no. 1, pp. 3–73, 1990.

[15] J. Osborne, "Notes on the use of data transformations," *Practical Assessment, Research and Evaluation*, vol. 8, pp. 1–8. 2002, doi: 10.7275/4vng-5608.

[16] M. H. Kutner, C. J. Nachtsheim, J. Neter, and W. Li, *Applied Linear Statistical Models*, 5th ed. New York: McGraw Hill, 2005.

[17] I. A. Iwok, "Seasonal modeling of Fourier series with linear trend," *International Journal of Statistics and Robability*, vol. 5, no. 6, pp. 65–72, 2016, doi: 10.5539/ijsp.v5n6p65.

[18] S. A. Delurgio, *Forecasting Principles and Applications*. New York: Mc Graw-Hill, 1998.

[19] A. C. Akpanta and I. S. Iwueze, "On applying the Bartlett transformation to time series data," *Journal of Mathematical Sciences*, vol. 20, no. 3, pp. 227–243, 2009.

[20] G. E. Box and D. R. Cox. "An analysis of

transformations," *Journal of the Royal Statistical Society: Series B (Methodological)*, vol. 26, no. 2, pp. 211–243, 1964, doi: 10.1111/j.2517-6161.1964.tb00553.x.

[21] H. Arsham and M. Lovric, "Bartlett's Test" in *International Encyclopedia of Statistical Science*. M. Lovric, Ed. Berlin, Germany: Springer, 2011, doi: 10.1007/978-3-642-04898-2_132.

[22] F. Bliemel, "Theil's forecast accuracy coefficient: A clarification" *Journal of Marketing Research*, vol. 10, no. 44, pp. 444–446, 1973, doi: https://doi.org/10.2307/3149394.

[23] Energy Policy and Planning office (EPPO), "Electricity Consumption for the Whole Country," 2021. [Online]. Available: http://www.eppo.go.th/index.php/th/energy-information/static-energy/static-electricity

[24] J. Pek, O. Wong, and A. C. Wong, "Data transformations for inference with linear regression: Clarifications and recommendations," *Practical Assessment, Research, and Evaluation*, vol. 22, no. 9, 2017, doi: 10.7275/2w3n-0f07.

[25] D. K. Lee, "Data transformation: A focus on the interpretation," *Korean Journal of Anesthesiology*, vol. 73, no. 6, pp. 503–508, 2020, doi: 10.4097/kja.20137.

[26] W. S. Cleveland and S. J. Devlin, "Locally weighted regression: An approach to regression analysis by local fitting," *Journal of the American Statistical Association*, vol. 83, no. 403, pp. 596–610, 1988, doi: 10.1080/01621459.1988.10478639.

[27] D. R. Gardner, "STL algorithm explained: STL Part II," 2017. [Online]. Available: http://www.gardner.fyi/blog/STL-Part-II/

[28] V. N. Vapnik, *The Nature of Statistical Learning Theory*, 2nd ed. Berlin, Germany: Springer, 2000.

[29] M. Awad and R. Khanna, "Support vector regression," in *Efficient Learning Machines*. Apress, California: Berkeley, 2015, pp. 67–80, doi: 10.1007/978-1-4302-5990-9_4.

[30] T. W. MacFarland and J. M. Yates, "Wilcoxon matched-pairs signed-ranks test," in *Introduction to Nonparametric Statistics for the Biological Sciences Using R*. Cham, Switzerland: Springer, 2016, pp. 133–175, doi: 10.1007/978-3-319-30634-6_5.